



**HAL**  
open science

## Evidence of transient amorphization during the polymorphic transformation of sorbitol induced by milling

Anthony Dupont, Mathieu Guerin, Florence Danede, Jean-François Willart

► **To cite this version:**

Anthony Dupont, Mathieu Guerin, Florence Danede, Jean-François Willart. Evidence of transient amorphization during the polymorphic transformation of sorbitol induced by milling. International Journal of Pharmaceutics, 2022, International Journal of Pharmaceutics, pp.121929. 10.1016/j.ijpharm.2022.121929 . hal-03707238

**HAL Id: hal-03707238**

**<https://hal.univ-lille.fr/hal-03707238>**

Submitted on 28 Jun 2022

**HAL** is a multi-disciplinary open access archive for the deposit and dissemination of scientific research documents, whether they are published or not. The documents may come from teaching and research institutions in France or abroad, or from public or private research centers.

L'archive ouverte pluridisciplinaire **HAL**, est destinée au dépôt et à la diffusion de documents scientifiques de niveau recherche, publiés ou non, émanant des établissements d'enseignement et de recherche français ou étrangers, des laboratoires publics ou privés.

*EVIDENCE OF TRANSIENT AMORPHIZATION  
DURING THE POLYMORPHIC TRANSFORMATION OF SORBITOL INDUCED BY MILLING*

A. Dupont, M. Guerain, F. Danède, J.F. Willart\*

<sup>1</sup>*Université de Lille, CNRS, INRAE, Centrale Lille, UMR 8207 – UMET – Unité Matériaux et Transformations, F-59000 Lille, France*

\*Corresponding author: [Jean-Francois.willart@univ-lille.fr](mailto:Jean-Francois.willart@univ-lille.fr)

## Abstract

In this paper, we show that the polymorphic transformation  $\gamma \rightarrow \alpha$  of sorbitol upon milling involves a transient amorphization of the material. This could be done by comilling sorbitol with a high T<sub>g</sub> amorphous material (Hydrochlorothiazide, T<sub>g</sub> = 115°C) to stabilize any transient amorphous fractions of sorbitol through the formation of a molecular alloy. The results indicate that for large sorbitol concentration (50%), the comilling leads to a heterogeneous mixture made of sorbitol crystallites in the form  $\alpha$  embedded into an amorphous molecular alloy sorbitol / HCT. Interestingly, the kinetic investigation of this transformation reveals that these two components are not produced simultaneously. On the contrary, they are produced one after the other, during two distinct consecutive stages. The first stage concerns the formation of the amorphous alloy while the second one concerns the polymorphic transformation  $\gamma \rightarrow \alpha$  of the fraction of crystalline sorbitol not involved in the alloy. These results clearly indicate that the polymorphic transformation of sorbitol upon milling results from the recrystallization of a transient amorphous state generated by the mechanical shocks. The investigations were mainly performed by calorimetry and powder X-ray diffraction.

## 1. Introduction

The properties of therapeutic molecular materials (mechanical properties, solubility and bioavailability for instance) strongly depend on their physical state which can be either crystalline or amorphous<sup>1-5</sup>. In the crystalline state, the polymorphic form of the material, i.e. the way the molecules are linked together and ordered by the hydrogen bonds, also influences these properties. The perfect control of the physical state of therapeutic materials during formulation processes is thus of prime interest.

In the pharmaceutical industry, milling is often used as a simple and effective way to reduce the grain sizes of powders<sup>6-9</sup>. However, it happens frequently that milling also induces phase transformations of these materials such as amorphization or polymorphic transformations<sup>10-12</sup>. It is now commonly accepted that the physical state of the material at the end of milling is closely correlated with its glass transition temperature<sup>10</sup>. An amorphization of these compounds is most often observed when the milling is carried out below the glass transition temperature of the material. Conversely, polymorphic transformations are generally observed when the milling is carried out above this temperature. This is for instance the case for sorbitol<sup>13,14</sup>, mannitol<sup>11</sup>, sulfamerazine<sup>15</sup>, glycine<sup>16</sup> or ranitidine hydrochloride<sup>17</sup>, for which polymorphic transformations upon milling have already been reported.

However, the mechanism underlying these polymorphic transformations is not yet clearly understood. Two explanations<sup>18</sup> oppose each other as to the mechanism involved. On the one hand, a transformation involving a sliding of the molecules along preferential crystallographic axes in the crystal lattice and a direct change of the crystal lattice of the initial form towards the crystal lattice of the final form is considered. On the other hand, a transient amorphization of the starting crystalline form of the material under shock, immediately followed by a recrystallization towards a metastable form. These two steps following a mechanical shock are expected to be extremely fast so that the intermediate amorphization step is very difficult to detect experimentally.

A promising way to better understand the mechanisms of transformations under milling is to study the kinetics of transformations which are the direct reflect of their underlying mechanism. However, up to now, only very few studies of these kinetics have been reported<sup>11,13,16</sup>. Recent works on mannitol<sup>11</sup> and sorbitol<sup>13</sup> have shown that polymorphic transformations upon milling are often characterized by a long induction time during which no transformation is detected, followed by a very rapid transformation from the initial form to the final form. A model of transformation in two stages was proposed to explain these specific kinetic features. It consists of a rapid amorphization of the impacted crystallites immediately followed by a rapid recrystallization toward a form which depends on the structural state of the neighbouring crystallites<sup>11,13</sup>. However, while this model accounts for the main characteristics of the kinetics, the reality of the transient amorphization stage was never clearly established. This is mainly due to the fact that amorphization fractions are very small and their life time very short making them hardly detectable.

We present here a study of the physical state changes of sorbitol during a comilling operation with an amorphous material. Sorbitol was used as the active ingredient because a previous study showed that it undergoes a polymorphic transformation under milling<sup>19</sup>. In addition, the kinetics of this transformation under milling has recently been studied in detail<sup>13</sup>. Sorbitol will be mixed here with Hydrochlorothiazide (HCT) which is a crystalline active ingredient at room temperature, but which has the advantage to form, easily and quickly, a stable amorphous substance under milling. The milling of sorbitol with HCT, which has a high glass transition temperature ( $T_g = 115^\circ\text{C}^{20}$ ), is expected to stabilize the amorphous sorbitol formed during milling and thus allow its detection. We will show in particular that the analysis of mixtures of different compositions after milling on the one hand, and the detailed

study of the kinetics of the polymorphic transformation on the other hand, provides essential indications concerning the fundamental mechanism at the origin of this transformation.

The structural state of milled material was investigated through combined X-ray diffraction and DSC experiments. The quantification of the amorphous fraction during milling was carried out with a diffraction method using an external standard.

## 2. Experimental

**Sorbitol** ( $C_6H_{14}O_6$ ) was purchased from Alfa Aesar (purity higher than 98%) and used without further purification. The structure of the molecule is shown in Figure 1. Sorbitol has a very rich polymorphism and 5 anhydrous crystalline forms have been identified:  $\alpha$ ,  $\beta$ ,  $\gamma$ ,  $\epsilon$  et  $\epsilon'$ <sup>21</sup>.

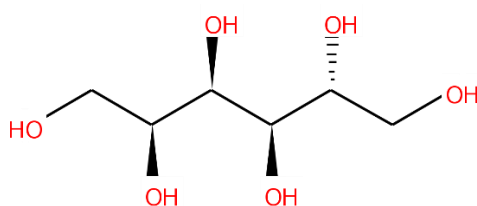


Figure 1 : Sorbitol molecule

The form  $\gamma$  is the most stable at room temperature. So far, only the structures of the  $\gamma$  and  $\alpha$  forms have been solved<sup>22,23</sup>. These two forms have orthorhombic structures, whose lattice parameters are summarized in Table 1. X-ray diffraction has revealed that the commercial powder we used is in the stable crystalline form  $\gamma$ <sup>23</sup>.

Table 1: Lattice parameters of the  $\gamma$  and  $\alpha$  forms of sorbitol<sup>22,23</sup>

Sorbitol	a (Å)	b (Å)	c (Å)	V (Å <sup>3</sup> )	Z
$\gamma$ form	24.301	20.572	4.867	2433	12
$\alpha$ form	8.677	9.311	9.727	785	4

**Hydrochlorothiazide** ( $C_7H_8ClN_3O_4S_2$ ) was purchased from Sigma Aldrich (purity higher than 99.9%) and used without any further purification. It is a diuretic of the thiazide family, widely used against arterial hypertension. The structure of the molecule is shown in Figure 2.

The literature mentions 4 polymorphic forms noted I, II, III and IV<sup>24</sup>. So far, only the structures of forms I (P2<sub>1</sub>)<sup>25</sup> and II (P2<sub>1</sub>/c)<sup>26</sup> have been resolved. Form I is the commercial form and the most stable form<sup>24</sup>.

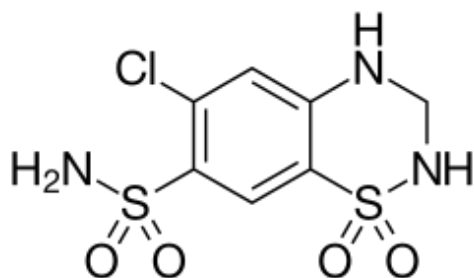


Figure 2 : Hydrochlorothiazide molecule

**The ball milling** was performed in a high energy planetary mill (Pulverisette 7-Fritsch) at room temperature. We used ZrO<sub>2</sub> milling jars of 43 cm<sup>3</sup> with seven balls (diameter 15 mm) of the same material. The rotation speed of the solar disk was set to 400 rpm which corresponds to an average acceleration of the milling balls of 5 g ( $g = 9.81 \text{ m.s}^{-2}$  is the acceleration of gravity). The milling times ( $t_m$ ) range between 0 min (non-milled material) and 50 hours.

**The Differential Scanning Calorimetry (DSC)** experiments were performed with a Q200 microcalorimeter of TA Instruments (Guyancourt, France). During all the measurements the calorimeter head was flushed with highly pure nitrogen gas. Temperature and enthalpy readings were calibrated using pure indium at the same scan rates used in the experiments. The samples have been placed in open pans (pan with no lid). For each scan a small amount ( $\approx 4 \text{ mg}$ ) of material was used to improve both the resolution and the thermal conductivity. Because sorbitol undergoes a strong chemical degradation above 110°C, the DSC scans of samples containing sorbitol have been stopped at this temperature.

**Powder X-ray diffraction experiments** were performed on a Panalytical XPert PRO diffractometer, equipped with a copper X-ray tube ( $\lambda=0.15406 \text{ nm}$ ) and a linear detector allowing acquisition of diffraction pattern from  $2\theta= 4^\circ$  to  $2\theta= 60^\circ$  with a scan step of  $0.0167^\circ/\text{s}$ . Powders are introduced in a sample holder (13 mm diameter and 2 mm depth) which rotate at a speed of 4 second for  $360^\circ$  in order to improve the statistics.

Structural analyses were carried out using Rietveld method on each diffraction diagram. It consists in calculating a theoretical diffraction pattern that fits best experimental data. Starting from a reference structure, a refinement of the various parameters of the simulated function is performed in order to minimize the weighted profile R-factor ( $R_{wp}$ ) defined by Equation (1):

$$R_{wp} = \left[ \frac{\sum_i [w_i (I_i^{exp} - I_i^{sim})^2]}{\sum_i (w_i I_i^{exp})^2} \right]^{1/2} \quad \text{Eq. 1}$$

with  $w_i = \frac{1}{\sqrt{I_i^{exp}}}$

where  $I_i^{exp}$  is the intensity of the experimental diffraction pattern at point i along the diffraction pattern and  $I_i^{sim}$  is the intensity of the simulated diffraction pattern at point i, depending on the crystal structure (lattice parameters, atomic positions, ...). For details on the simulation of the diffraction pattern, see <sup>27</sup>. It is generally considered that a  $R_{wp}$  ratio below 10 % is acceptable. The  $I_i^{exp}$  peak

position and shape depend on lattice parameters and structural defects. In particular, the width of the diffraction peaks is the parameter that contains information about the average crystallite size and the microstrain of constitutive crystals. These structural parameters can be included in the simulation profile and optimized to match the experimental diagram. For each diagram, two refinements were performed from slightly different starting parameters to evaluate the robustness of the resulting solution. The reference structures and the starting parameters  $I_i^{sim}$  used for the calculation were those determined by Rukiah et al.<sup>22</sup> for the  $\gamma$  form of the sorbitol and Park et al.<sup>23</sup> for the  $\alpha$  form. Rietveld analyses were carried out with the MAUD<sup>28</sup> software on the whole diagram. It has to be noted that the diffractometer set-up contributes to both broadening and intensity of the diffraction peaks. This contribution, called the instrumental function, was independently determined with the Rietveld analysis using NAC and silicon references. It was then implemented in MAUD and used to determine structural parameters of the crystals.

The Rietveld method also allows the quantification of the percentage of crystalline phase for each species present in a crystalline mixture, since they influence the relative intensity of their respective diffraction peaks. The amount of amorphous phase in the material is analysed using the external standard method<sup>29</sup>. An external standard is mixed in a known proportion with the material after milling. The amount of amorphous phase is then determined using the following equation:

$$W_a = 1 - \frac{W_s}{W_{s,calc.}} \quad \text{Eq. 2}$$

$W_a$  is the percentage of amorphous phase,  $W_s$  is the phase percentage of the material chosen as a standard and  $W_{s,calc.}$  is the percentage of phase of this standard determined by the Rietveld method in the mixture. In the present investigations, 5 % of silicon used as standard has been mixed to samples before X-ray diffraction experiments. Details on the application of this method and its validation in the context of this work are presented in supplementary information.

### 3. Results and analysis

#### a. Effects of milling on the structural state of sorbitol/HCT physical mixtures

Figure 3 shows the diffractograms of pure sorbitol and pure HCT recorded before and after a 50-hour milling process. Before milling, sorbitol shows Bragg peaks characteristic of the crystalline form  $\gamma$  while after milling it shows those characteristic of the crystalline form  $\alpha$  (see supplementary information for reference patterns). This indicates that sorbitol has undergone a total polymorphic transformation  $\gamma \rightarrow \alpha$  during the milling process in agreement with what has been previously reported in the literature<sup>13,14</sup>. For HCT, the situation is different. The Bragg peaks characteristic of the crystalline state observed before milling have disappeared after milling. This reveals a total amorphization of HCT upon milling.

Figure 3 also shows X-ray diffraction patterns of physical mixtures sorbitol / HCT recorder after 50 hours of milling for sorbitol fractions  $X_{sorb} = 0.20$  and  $X_{sorb} = 0.50$ . For  $X_{sorb} = 0.20$ , the diffractogram shows a diffusion halo without any Bragg peak. This indicates that both HCT and sorbitol have been totally amorphized during comilling. For  $X_{sorb} = 0.50$ , the diffractogram shows many small Bragg peaks corresponding to the form  $\alpha$  of sorbitol which superimpose on a smaller diffusion halo. No Bragg peaks corresponding to crystalline HCT or to the initial form  $\gamma$  of sorbitol can be detected. This indicates that HCT has been totally amorphized and that only a part of sorbitol has been amorphized while the other part has undergone a polymorphic transformation  $\gamma \rightarrow \alpha$  during the comilling. It must be noted that in

all cases no evolution of the X-ray diffraction pattern could be observed for longer milling, which indicates that a stationary state has been reached.

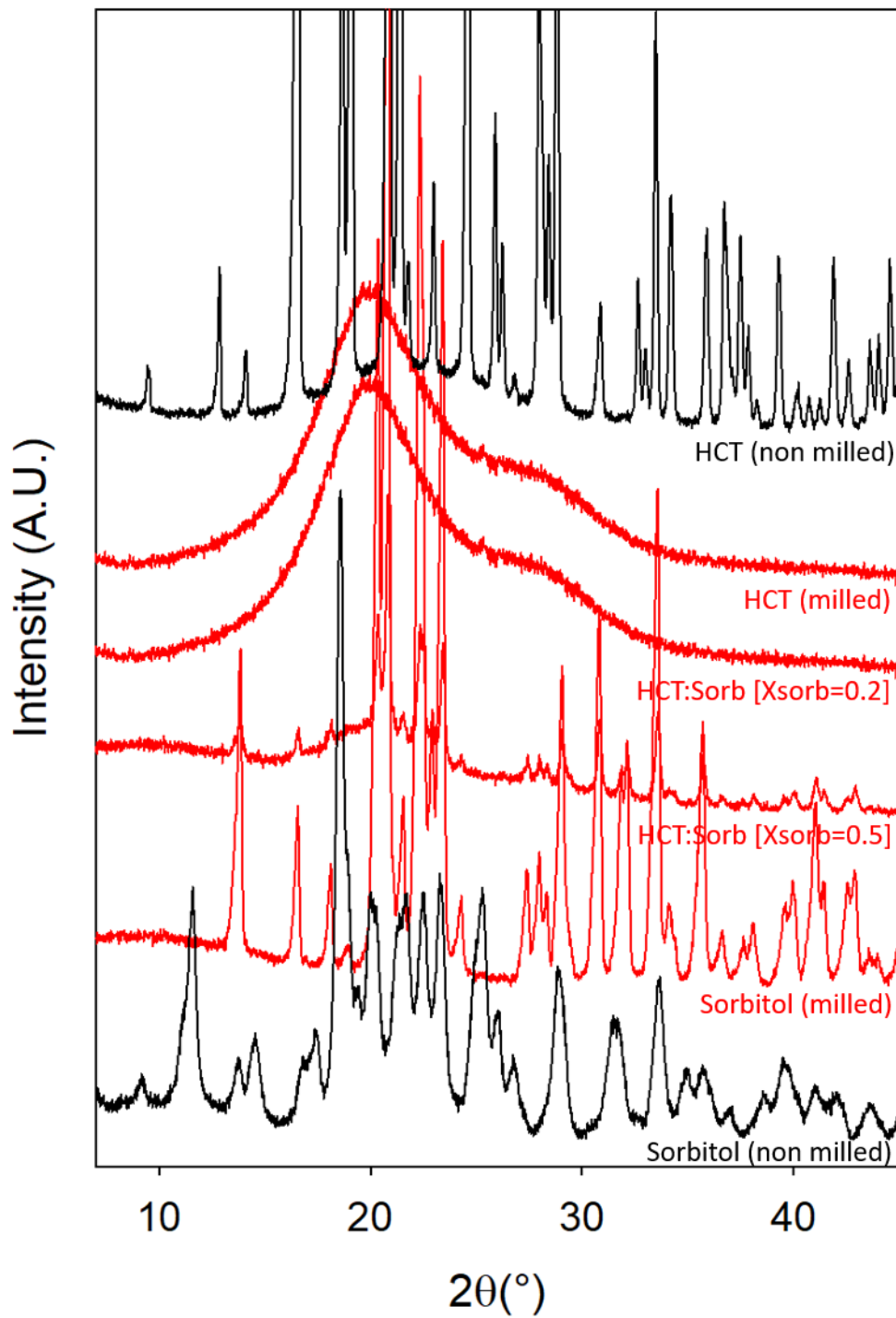


Figure 3 : X-ray diffraction patterns of non-milled crystalline HCT, non-milled crystalline sorbitol ( $\gamma$  form) and HCT-sorbitol mixtures with 0, 20, 50 and 100% of sorbitol recorded after 50 hours of milling. The patterns of milled materials are in red while those of non-milled materials are in black

Figure 4 shows heating (5°C/min) DSC scans of comilled (50 h) physical mixtures sorbitol / HCT for sorbitol fractions ranging from  $X_{\text{sorb}} = 0.00$  to  $X_{\text{sorb}} = 0.50$ . For pure HCT ( $X_{\text{sorb}} = 0.00$ ) the thermogram shows a Cp jump at  $T_g = 115^\circ\text{C}$  characteristic of the glass transition of HCT and, at higher temperature, a recrystallization exotherm. These events indicate that the HCT underwent a crystal to glass transformation during the milling in coherence with the X-ray diffraction analysis (Figure 3). For  $X_{\text{sorb}} = 0.05$  to 0.25, the thermograms still show a single Cp jump which shifts noticeably toward low temperature for increasing sorbitol fractions. This single character of the glass transition indicates that milling has induced a coamorphization of sorbitol and HCT, i.e. the formation of a homogeneous amorphous alloy characterized by a single relaxation time. Moreover, the decrease of  $T_g$  indicates that sorbitol has a plasticizing effect on HCT, in coherence with its glass transition temperature ( $T_g = -3^\circ\text{C}$ )<sup>30</sup> much lower than that of HCT ( $T_g = 115^\circ\text{C}$ )<sup>20</sup>. We can also note that the recrystallization of HCT seen in the pure compound upon heating also occurs in the mixtures in a temperature range which decreases

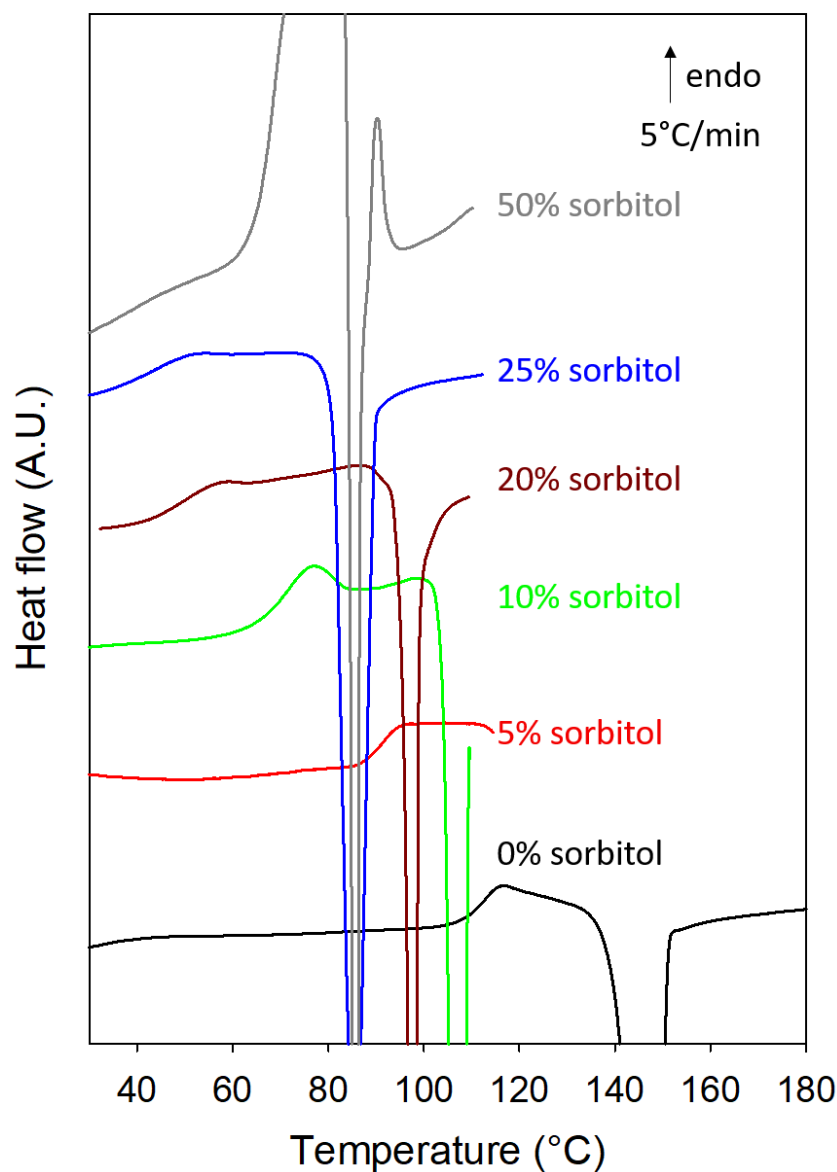


Figure 4: Heating DSC scans of HCT-sorbitol mixtures containing 0-50% sorbitol milled 50 hours



in parallel with  $T_g$ . This recrystallization does not concern sorbitol as it occurs above its melting point. For  $X_{\text{sorb}} > 0.25$  (e.g.  $X_{\text{sorb}} = 0.5$ ), the glass transition stops shifting and its amplitude decreases rapidly, making it difficult to observe. These two facts indicate respectively that the composition of the amorphous alloy becomes stationary and that the total amorphous fraction in the overall sample decreases. This behaviour suggests that the sorbitol fractions exceeding 25 % do not coamorphize with the HCT and remain in a crystalline state. The sample then appears to be a physical mixture made of crystallites of sorbitol dispersed into a homogeneous amorphous alloy HCT / sorbitol containing about 25 % of amorphous sorbitol. This result is consistent with the X-ray diffraction analysis of the comilled mixtures (see Figure 3) which shows the persistence of a crystalline component of the form  $\alpha$  of sorbitol for  $X_{\text{sorb}} = 0.50$ . Above  $T_g$ , the thermograms show the endothermic melting of the form  $\alpha$  of sorbitol which overlaps the recrystallization of HCT.

The comilling of HCT/sorbitol mixtures therefore leads to a homogeneous amorphous alloy for sorbitol fractions below  $X_{\text{sorb}} = 0.25$ , which shows unambiguously that crystalline sorbitol can be amorphized by milling. Obtaining this type of alloy by the usual melting-quenching of the physical crystalline mixture is impossible since sorbitol degrades on heating well before reaching the melting temperature of HCT ( $T_m = 267^\circ\text{C}$ )<sup>20</sup>. The possibility to coamorphize the two compounds directly in the solid state makes it possible to establish part of the Gordon Taylor curve of the HCT / sorbitol mixture ( $T_g(X_{\text{sorb}})$ ) in the sorbitol concentration range where the coamorphization is total. This curve is reported in Figure 5, using the  $T_g$  values derived from the thermograms presented in figure 4.

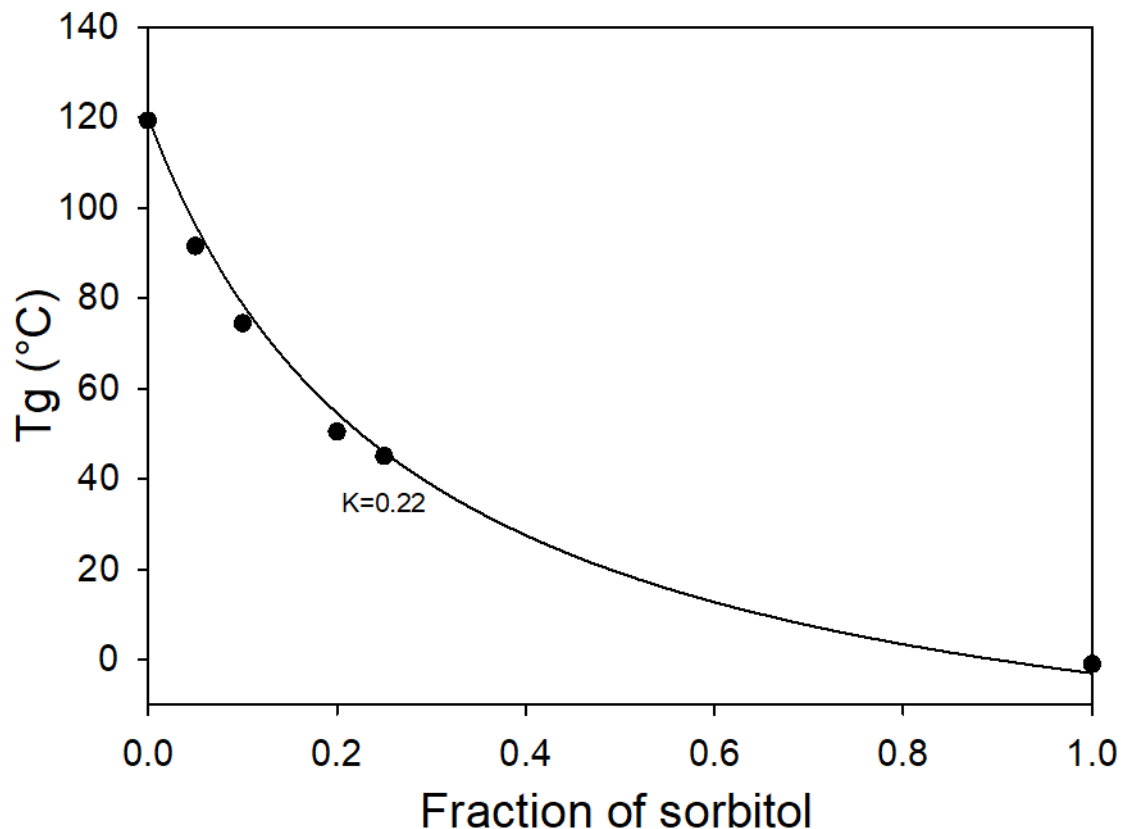


Figure 5 : Evolution of the glass transition temperature as a function of the sorbitol fraction. The black line curve corresponds to the best fit ( $K=0.22$ ) of Gordon Taylor's law (Eq. 3) on the data.

The glass transition temperature of pure sorbitol obtained by quenching the liquid is also reported. The black line corresponds to the best fit of the experimental data by the Gordon Taylor curve (Equation 3) generally used to describe this type of evolution:

$$T_g = \frac{X_{sorb}T_g^{sorb} + K(1-X_{sorb})T_g^{HCT}}{X_{sorb} + (1-X_{sorb})} \quad \text{Eq. 3}$$

In this equation,  $T_g^{sorb}$  and  $T_g^{HCT}$  are the glass transition temperatures of the pure compounds,  $X_{sorb}$  is the fraction of sorbitol in the mixture and K is a fitting parameter describing the curvature of the evolution. The best fit was obtained for  $K=0.22$  and perfectly describes the experimental evolution of  $T_g$  with the composition.

The Gordon Taylor curve, indicates that the comilling of physical HCT/sorbitol mixtures leads to a homogeneous amorphous alloy only for sorbitol concentrations below 25%, i.e. when the glass transition temperature of the expected alloy is above 40°C. It is interesting to note that this temperature is close to the effective temperature at which the milling takes place. Indeed, thermosensitive stickers glued to the outside of the jar showed that the temperature of the jar during the milling varies between 30 and 40°C due to the mechanical heating induced by the shocks of the balls. It can therefore be thought that the transformation of the mixture under milling is governed by a competition between a mechanism of mechanical coamorphization and a mechanism of conventional thermally activated recrystallization. For low sorbitol concentrations ( $X_{sorb} \leq 0.25$ ), the  $T_g$  of the alloy remains much higher than the milling temperature so that the recrystallization mechanism is almost inactive due to the low molecular mobility below  $T_g$ . In this case, a total coamorphization of the mixture is achieved. Conversely, for higher sorbitol concentrations ( $X_{sorb} > 0.25$ ), the  $T_g$  of the forming alloy approaches the milling temperature so that the molecular mobility becomes sufficient to allow the recrystallization of sorbitol and thus counterbalance the mechanical amorphization. In this case, the milled sample reaches a heterogeneous stationary state consisting of an amorphous alloy whose  $T_g$  is close to the effective milling temperature, and of a crystalline fraction of sorbitol coming from the recrystallization of the supersaturated alloy.

This recrystallization could explain why the crystalline fraction present at the end of milling is in the form  $\alpha$ . However, it is also possible that the form  $\alpha$  comes directly from the milling of the crystallites of form  $\gamma$  not yet coamorphized or which would have recrystallized toward the form  $\gamma$ . The fact that for  $X_{sorb} > 0.25$ , comilling induces both a coamorphization of one part of the sorbitol and a polymorphic transformation of the other part, provides a particularly interesting situation for testing the existence of a transient amorphization during polymorphic transformations under milling. The kinetic study of the evolution of the different structural components (amorphous alloy,  $\alpha$  form and  $\gamma$  form) should make it possible to determine, in particular, whether amorphization and polymorphic transformations occur in parallel or follow one another.

## b. Kinetics of the transformation of sorbitol during the comilling of a physical mixture

We have determined the temporal evolution of the structural composition of sorbitol during the comilling process of a physical mixture HCT / sorbitol for  $X_{sorb} = 0.50$ . The structural composition of

sorbitol has been determined by powder X-ray diffraction analysis. To get rid of HCT Bragg peaks and make the structural analysis of sorbitol easier and more precise, HCT was used in the amorphous form previously obtained by a 10-hour milling of the pure compound. Sorbitol was used in the crystalline form  $\gamma$ . It has been checked that the structural state (crystalline or amorphous) of HCT in the initial physical mixture has no influence on the structural state of the mixture reached after a 50-hour milling process. Similarly, increasing the rotation speed of the planetary mill makes the structural changes more rapid but does not change the structural composition of the final state.

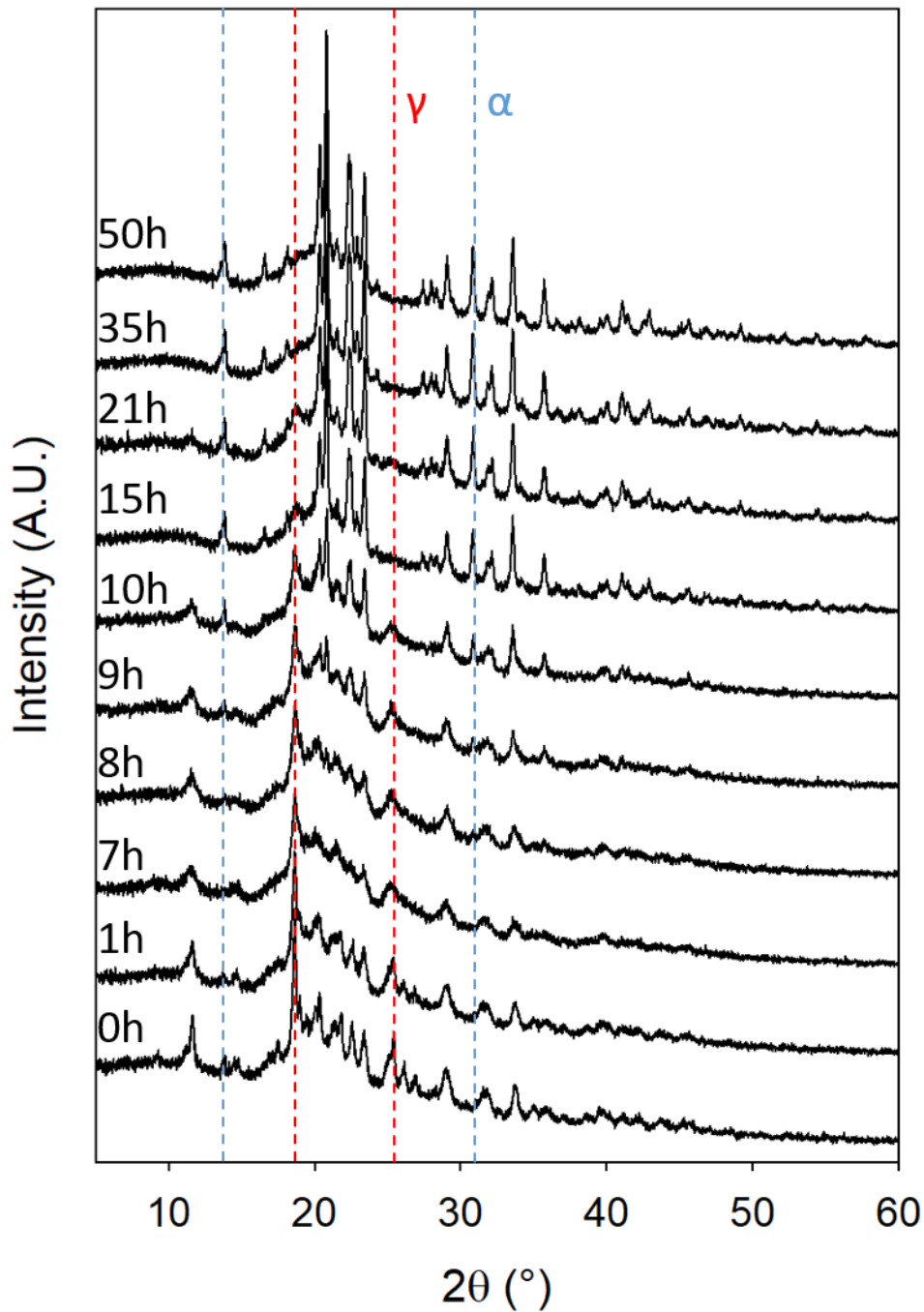


Figure 6 : Diffractograms of the sorbitol / HCT 50/50 mixture recorded after different milling times varying from 0 to 50h. The milling times are indicated above each thermogram.

Figure 6 shows the x-ray diffraction patterns of the physical mixture recorded after different milling times ranging from 0 to 50 h. At  $t = 0$  h, the diffractogram is that expected for the initial physical mixture. In particular, it shows Bragg peaks characteristic of the form  $\gamma$  of sorbitol superimposed to a noticeable halo of diffusion corresponding to the 50% of amorphous HCT. From  $t = 1$  h to  $t = 8$  h, very little evolution is observed. Both the halo of diffusion and the Bragg peaks of the form  $\gamma$  persist. We can however notice a broadening of these Bragg peaks which reveals a strong crystallite size reduction due to the mechanical impacts. Between 9 and 35 hours of milling deep changes of the X-ray diffraction pattern can be observed. The Bragg peaks characteristic of the form  $\gamma$  disappear progressively while those characteristic of the form  $\alpha$  develop. After 35 hours of milling the Bragg peaks characteristic of the form  $\gamma$  have totally disappeared and no more evolution of the X-ray diffraction pattern is observed for longer milling (e.g. 50 h). These results thus reveal that the transformation  $\gamma \rightarrow \alpha$  upon comilling appears to be completed within 35 hours.

Rietveld analyses of the X-ray diffraction patterns of figure 6 allows the determination of the percentage of forms  $\alpha$  and  $\gamma$  in the material after each milling times. The kinetics of the polymorphic transformation of sorbitol upon milling derived from these results is shown in Figure 7. It is compared to the kinetics of transformation of pure sorbitol determined in previous works<sup>13</sup>. It appears clearly that the transformation is much slower in the mixture than in the pure compound. This is due to both a longer induction time (8 hours instead of 2 hours) and a smaller transformation rate in the effective subsequent transformation stage which lasts more than 10 hours instead of 1 hours.

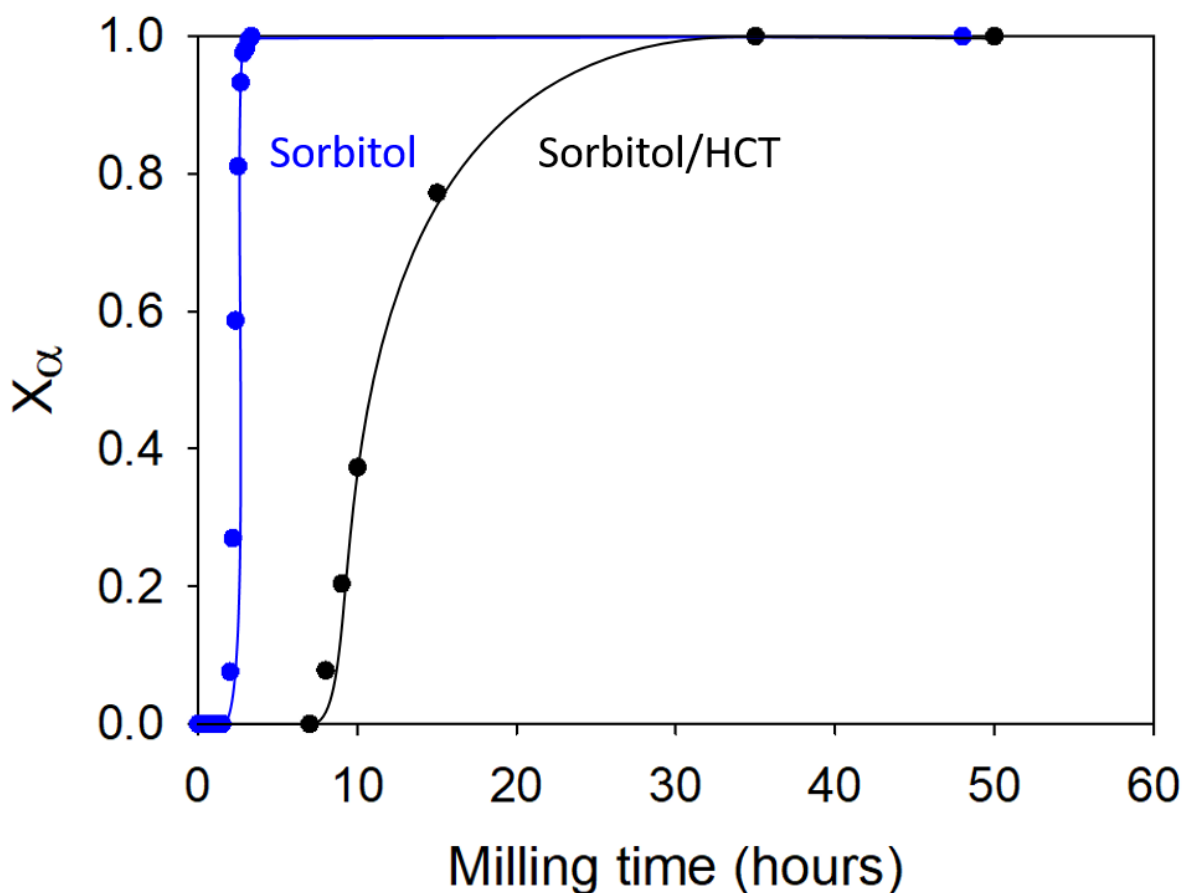


Figure 7 : Kinetics of transformation of sorbitol in the HCT-sorbitol mixture (black curve) during milling. The kinetics of transformation of pure sorbitol during milling in the same conditions (blue curve) is also reported for comparison (data drawn from<sup>13</sup>).

The comilled samples of figure 6 were then reinvestigated by powder X-ray diffraction after adding  $W_s = 5\%$  of silicon, in order to determine their amorphous fraction. The Rietveld analysis of the new diffractograms allows to determine the calculated percentage of silicon  $W_{s,calc}$  and thus, the amorphous content of the mixture using equation 2 (please see experimental section). Using this method, the amorphous content ( $X_{am}$ ) of the mixture was quantified after the different milling times (see supplementary information).

From this quantification, Figure 8 summarizes the temporal evolution of the fractions of the different physical forms (form  $\alpha$ , form  $\gamma$  and amorphous form) of sorbitol during the 50 hours of milling. Three main stages can be clearly distinguished:

- (i) During the first hour of milling, 40% of the initial crystalline sorbitol (form  $\gamma$ ) coamorphizes with the amorphous HCT, while no sign of the form  $\alpha$  of sorbitol can be detected. This indicates that sorbitol amorphizes upon milling and that this amorphization stage precedes any polymorphic transformation toward the form  $\alpha$ .
- (ii) Between 1 and 10 h of milling, the coamorphization process stops and no change of the structural composition of sorbitol can be detected during this stage. As explained in section a), the stopping of the coamorphization process is due to the increasing plasticization of the alloy by sorbitol in the previous stage which increases its molecular mobility, and thus, its propension to recrystallize. This results in a competition between coamorphization and recrystallisation of sorbitol toward the form  $\gamma$  which leads to an apparent stationary structural composition. The coamorphization of sorbitol is thus not really stopped, but rather counterbalanced by its recrystallization.
- (iii) Beyond 10 h of milling the fraction of form  $\gamma$  drops from 0.6 to 0 while that of form  $\alpha$  increases from 0 to 0.6. These two evolutions occur in parallel while the amorphous fraction remains constant which leads to an apparent conversion of the  $\gamma$  form toward the  $\alpha$  form. However, it is likely that this mechanism is in fact the continuation of that governing the previous stage, except that the recrystallization now occurs toward the form  $\alpha$  instead of the form  $\gamma$ . The disappearance of the form  $\gamma$  would thus be due to its coamorphization with the alloy, while the development of the form  $\alpha$  would result from the recrystallization of the amorphous sorbitol involved in this alloy.

The passage from stage (ii) to stage (iii) is thus triggered by a change in the nature of the recrystallization of amorphous fractions (toward form  $\gamma$  in stage (ii) and toward form  $\alpha$  in stage (iii)). This change was already detected during the milling of the pure compound<sup>13</sup> and was attributed to a microstructural effect. As explained in more details in reference<sup>13</sup>, the recrystallization of an amorphous grain is strongly oriented by the crystalline state of adjacent crystallites. In the early stage of milling, sorbitol crystallites are mainly in the form  $\gamma$ . As a result, emerging crystallites  $\alpha$  are mainly surrounded by crystallites  $\gamma$ , so that they are likely to return toward the form  $\gamma$  after the next amorphizing impact. The conditional recrystallization thus leads, in the early stages of milling, to a stationary state consisting of a small fraction of evanescent crystallites  $\alpha$  dispersed among a multitude of crystallites  $\gamma$ . This situation persists until the accidental formation of a cluster of crystallites  $\alpha$ . The crystallites  $\alpha$  involved in this cluster are much more stable than the isolated crystallites  $\alpha$  because each of them is in contact with several other crystallites  $\alpha$ . This stable cluster then develops, as it promotes the recrystallization of the amorphous grains that are in contact with it, towards the form  $\alpha$ . Such a

mechanism was shown to account for the succession of an induction stage and a transformation stage in the pure compound. It is expected to also hold during the comilling of the physical mixture amorphous HCT / crystalline- $\gamma$ -sorbitol.

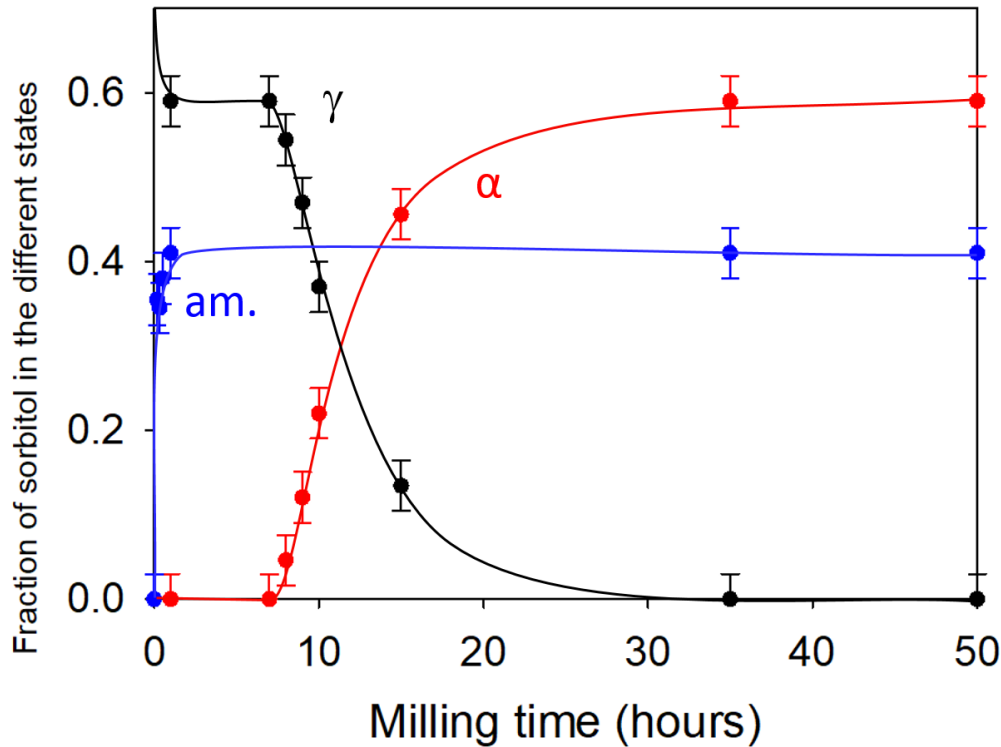


Figure 8 : Temporal evolution of the different physical forms of sorbitol (form  $\gamma$ , form  $\alpha$  and amorphous form) during a 50-hour comilling process

However, in this latter case, due to the partial formation of an amorphous HCT/sorbitol alloy in the very early stages of milling, the crystallites  $\alpha$  are dispersed among both crystallites  $\gamma$  and amorphous mixture grains. This greater dispersion significantly reduces the probability of forming a stable cluster of  $\alpha$ -crystallites, which is expected to increase the induction time required to form this cluster. This increase in induction time can be seen in Figure 7. It is only 2 hours for the milled pure sorbitol versus 8 hours for the milled mixture sorbitol  $\gamma$  / amorphous HCT. Similarly, the presence of some amorphous grains at the interface of the stable cluster decreases the growth rate of this cluster. That is why, the transformation stage of pure sorbitol is very short (less than one hour) compared to that of the mixture sorbitol  $\gamma$  / amorphous HCT (Figure 7 and Figure 8). The presence of a permanent fraction of amorphous grains in the system is thus at the origin of a greater isolation of the crystallites which delays the formation of a stable cluster of crystallites  $\alpha$  and slows down the transformation  $\gamma \rightarrow \alpha$  which follows it.

## 4. Conclusion

The objective of this paper was to determine if polymorphic transformations induced by milling are direct, or if they involved, on the contrary, a transient amorphization stage. This open question was here addressed through a detailed kinetics study of the physical transformations of crystalline  $\gamma$ -sorbitol during a long comilling process with amorphous hydrochlorothiazide.

The results indicate that the comilling leads to a heterogeneous stationary state made of two components. The first one is crystalline  $\alpha$ -sorbitol which indicates that part of the initial  $\gamma$ -sorbitol has undergone a polymorphic transformation identical to that observed during the milling of the pure compound<sup>13</sup>. The second component is a homogeneous amorphous molecular alloy made of sorbitol and HCT. It reveals that sorbitol can be amorphized upon milling. Moreover, the kinetics analysis of the structural composition of sorbitol during the whole milling process indicates that the two components do not form in parallel but, on the contrary, during two totally separated stages. In the first stage,  $\gamma$ -sorbitol is progressively amorphized and stabilized by mixing with HCT. The second stage starts when the increasing plasticizing effect of sorbitol allows its recrystallization which then occurs toward the form  $\alpha$ .

These results prove that the polymorphic transformation  $\gamma \rightarrow \alpha$  of pure sorbitol upon milling results from the combination of two successive physical changes: An amorphization of  $\gamma$ -crystallites due to the mechanical chocs, followed by a classical thermally activated recrystallisation toward the form  $\alpha$ . Because the recrystallization process is very fast, the transient amorphous fraction was never detected so far. However, this transient amorphous state could be clearly identified in the present study by stabilization with a high  $T_g$  amorphous compound (HCT) during comilling experiments.

This paper thus provides a new strategy to get direct proofs of the transient amorphisation which possibly occurs during polymorphic transformations upon milling. This strategy has the advantage to be general so that it can potentially be applied to any compound. It would thus be interesting to use this approach with many other drugs undergoing polymorphic transformations upon milling (mannitol, sulfamerazine, glycine, ranitidine...) to test the general character of this mechanism.

The paper also gives, by the way, important information on the temporal evolution of the physical state of physical mixtures during a comilling process and, in particular, the order of appearance of the different physical forms (co-amorphous state and polymorphic forms).

## Acknowledgements

One of us (A.D.) thanks the region Hauts-de-France for the financial support which allowed him to conduct its PhD thesis and the present work.

## Captions

Figure 1: Sorbitol molecule

Figure 2: Hydrochlorothiazide molecule

Figure 3: X-ray diffraction patterns of non-milled crystalline HCT, non-milled crystalline sorbitol ( $\gamma$  form) and HCT-sorbitol mixtures with 0, 20, 50 and 100% of sorbitol recorded after 50 hours of milling. The patterns of milled materials are in red while those of non-milled materials are in black

Figure 4: Heating DSC scans of HCT-sorbitol mixtures containing 0-50% sorbitol milled 50 hours

Figure 5: Evolution of the glass transition temperature as a function of the sorbitol fraction. The black line curve corresponds to the best fit ( $K=0.22$ ) of Gordon Taylor's law (Eq. 3) on the data.

Figure 6: Diffractograms of the sorbitol / HCT 50/50 mixture recorded after different milling times varying from 0 to 50h. The milling times are indicated above each thermogram.

Figure 7: Kinetics of transformation of sorbitol in the HCT-sorbitol mixture (black curve) during milling. The kinetics of transformation of pure sorbitol during milling in the same conditions (blue curve) is also reported for comparison (data drawn from<sup>13</sup>).

Figure 8: Temporal evolution of the different physical forms of sorbitol (form  $\gamma$ , form  $\alpha$  and amorphous form) during a 50 hour comilling

Table 1: Lattice parameters of the  $\gamma$  and  $\alpha$  forms of sorbitol <sup>22,23</sup>



## References

1. Brittain, H. G. Effects of mechanical processing on phase composition. *J. Pharm. Sci.* **91**, 1573–1580 (2002).
2. Davey, R. J. Polymorphism in Molecular Crystals Joel Bernstein. Oxford University Press, New York, 2002. ISBN 0198506058. *Cryst. Growth Des.* **2**, 675–676 (2002).
3. Blagden, N., de Matas, M., Gavan, P. T. & York, P. Crystal engineering of active pharmaceutical ingredients to improve solubility and dissolution rates. *Adv. Drug Deliv. Rev.* **59**, 617–630 (2007).
4. Murdande, S. B., Pikal, M. J., Shanker, R. M. & Bogner, R. H. Solubility advantage of amorphous pharmaceuticals: I. A thermodynamic analysis. *J. Pharm. Sci.* **99**, 1254–1264 (2010).
5. Hancock, B. C. & Parks, M. What is the True Solubility Advantage for Amorphous Pharmaceuticals? *Pharm. Res.* **17**, 397–404 (2000).
6. Loh, Z. H., Samanta, A. K. & Sia Heng, P. W. Overview of milling techniques for improving the solubility of poorly water-soluble drugs. *Asian J. Pharm. Sci.* **10**, 255–274 (2015).
7. Kipp, J. E. The role of solid nanoparticle technology in the parenteral delivery of poorly water-soluble drugs. *Int. J. Pharm.* **284**, 109–122 (2004).
8. Merisko-Liversidge, E. & Liversidge, G. G. Nanosizing for oral and parenteral drug delivery: A perspective on formulating poorly-water soluble compounds using wet media milling technology. *Adv. Drug Deliv. Rev.* **63**, 427–440 (2011).
9. Liversidge, G. G. & Cundy, K. C. Particle size reduction for improvement of oral bioavailability of hydrophobic drugs: I. Absolute oral bioavailability of nanocrystalline danazol in beagle dogs. *Int. J. Pharm.* **125**, 91–97 (1995).
10. Willart, J. F. & Descamps, M. Solid State Amorphization of Pharmaceuticals. *Mol. Pharm.* **5**, 905–920 (2008).
11. Martinetto, P. *et al.* Structural Transformations of d-Mannitol Induced by in Situ Milling Using Real Time Powder Synchrotron Radiation Diffraction. *Cryst. Growth Des.* **17**, 6111–6122 (2017).
12. Latreche, M., Willart, J.-F., Guerin, M., Hédoux, A. & Danède, F. Using Milling to Explore Physical States: The Amorphous and Polymorphic Forms of Sulindac. *J. Pharm. Sci.* **108**, 2635–2642 (2019).
13. Dupont, A. *et al.* Kinetics and mechanism of polymorphic transformation of sorbitol under mechanical milling. *Int. J. Pharm.* **590**, 119902 (2020).
14. Willart, J.-F. *et al.* Polymorphic transformation of the  $\Gamma$ -form of d-sorbitol upon milling: structural and nanostructural analyses. *Solid State Commun.* **135**, 519–524 (2005).
15. Macfionnghaile, P. *et al.* Effects of Ball-Milling and Cryomilling on Sulfamerazine Polymorphs: A Quantitative Study. *J. Pharm. Sci.* **103**, 1766–1778 (2014).
16. Matsuoka, M., Hirata, J. & Yoshizawa, S. Kinetics of solid-state polymorphic transition of glycine in mechano-chemical processing. *Chem. Eng. Res. Des.* **88**, 1169–1173 (2010).
17. Chieng, N., Zujovic, Z., Bowmaker, G., Rades, T. & Saville, D. Effect of milling conditions on the

- solid-state conversion of ranitidine hydrochloride form 1. *Int. J. Pharm.* **327**, 36–44 (2006).
18. De Gusseme, A., Neves, C., Willart, J. F., Rameau, A. & Descamps, M. Ordering and disordering of molecular solids upon mechanical milling: The case of fananserine. *J. Pharm. Sci.* **97**, 5000–5012 (2008).
  19. Willart, J.-F. *et al.* Polymorphic transformation of the  $\Gamma$ -form of d-sorbitol upon milling: structural and nanostructural analyses. *Solid State Commun.* **135**, 519–524 (2005).
  20. Ruponen, M., Rusanen, H. & Laitinen, R. Dissolution and Permeability Properties of Co-Amorphous Formulations of Hydrochlorothiazide. *J. Pharm. Sci.* **109**, 2252–2261 (2020).
  21. Nezzal, A., Aerts, L., Verspaille, M., Henderickx, G. & Redl, A. Polymorphism of sorbitol. *J. Cryst. Growth* **311**, 3863–3870 (2009).
  22. Rukiah, M., Lefebvre, J., Hernandez, O., Van Beek, W. & Serpelloni, M. Ab initio structure determination of the  $\Gamma$  form of D-sorbitol (D-glucitol) by powder synchrotron X-ray diffraction. *J. Appl. Crystallogr.* **37**, 766–772 (2004).
  23. Park, Y. J., Jeffrey, G. A. & Hamilton, W. C. Determination of the crystal structure of the A form of D-glucitol by neutron and X-ray diffraction. *Acta Crystallogr. Sect. B Struct. Crystallogr. Cryst. Chem.* **27**, 2393–2401 (1971).
  24. Kim, B. H. & Kiln, J. K. *Pharmaceutical Studies on the Polymorphism of Hydrochlorothiazide.* *Arch. Pharm. Res* vol. 7 (1984).
  25. Dupont, L. & Dideberg, O. Structure cristalline de l'hydrochlorothiazide, C 7 H 8 ClN 3 O 4 S 2 . *Acta Crystallogr. Sect. B Struct. Crystallogr. Cryst. Chem.* **28**, 2340–2347 (1972).
  26. Florence, A. *et al.* Powder study of hydrochlorothiazide form II. *Acta Crystallogr. Sect. E Struct. Reports Online* **61**, o2798–o2800 (2005).
  27. Paufler, P. R. A. Young (ed.). *The Rietveld Method.* International Union of Crystallography. Oxford University Press 1993. 298 p. ISBN 0–19–855577–6. *Cryst. Res. Technol.* **30**, 494–494 (1995).
  28. Lutterotti, L. Total pattern fitting for the combined size–strain–stress–texture determination in thin film diffraction. *Nucl. Instruments Methods Phys. Res. Sect. B Beam Interact. with Mater. Atoms* **268**, 334–340 (2010).
  29. Madsen, I. C., Scarlett, N. V. Y. & Kern, A. Description and survey of methodologies for the determination of amorphous content via X-ray powder diffraction. *Zeitschrift für Krist.* **226**, 944–955 (2011).
  30. Yu, L. Growth Rings in d-Sorbitol Spherulites: Connection to Concomitant Polymorphs and Growth Kinetics. *Cryst. Growth & Des.* **3**, 967–971 (2003).